*Article*

# Evaluation of Thermodynamic Parameters for Cu(II) Ions Biosorption on Algae Biomass and Derived Biochars

**Alina Alexandra Ciobanu [1], Dumitru Bulgariu [2,3], Ioana Alexandra Ionescu [4], Diana Maria Puiu [4], Gabriela Geanina Vasile [4] and Laura Bulgariu [1,\*]**

[1] Department of Environmental Engineering and Management, "Cristofor Simionescu" Faculty of Chemical Engineering and Environmental Protection, Technical University Gheorghe Asachi of Iasi, 700050 Iaşi, Romania; alina-alexandra.ciobanu@student.tuiasi.ro

[2] Department of Geology, Faculty of Geography and Geology, "Al.I.Cuza" University of Iaşi, 700050 Iaşi, Romania; dbulgariu@yahoo.com

[3] Romanian Academy, Filial of Iaşi, Branch of Geography, 700050 Iaşi, Romania

[4] National Research and Development Institute for Industrial Ecology, 060652 Bucharest, Romania; ioana.ionescu@incdecoind.ro (I.A.I.); diana.puiu@incdecoind.ro (D.M.P.); gabriela.vasile@incdecoind.ro (G.G.V.)

\* Correspondence: lbulg@ch.tuiasi.ro

**Abstract:** The removal of metal ions by biosorption on inexpensive materials is still a challenge for environmental engineering research. In this study, marine green algae biomass (*Ulva lactuca* sp.) and the biochars obtained from this biomass, at 320 °C (BC-320) and 550 °C (BC-550), were used as biosorbents for the removal of Cu(II) ions from aqueous solution. In addition to comparing the biosorption capacities, the determination of the thermodynamic parameters allows the choice of the most suitable material for the biosorption processes. The experimental results, obtained for Cu(II) ions biosorption on each biosorbent (algae biomass (AB), BC-320 and BC-550), at three different temperatures (10, 30 and 50 °C) were analyzed using Langmuir and Freundlich isotherm models, while pseudo-first order, pseudo-second order and intra-particle diffusions models were used to model the kinetic data. The biosorption of Cu(II) ions is best described by the Langmuir model and the pseudo-second kinetic model, regardless of the type of biosorbent. Such behavior is characteristic for the retention of metal ions on low-cost materials, and is explained in the literature using the concepts of molecular symmetry. The maximum biosorption capacity ($q_{max}$, mg/g) depends on the temperature, but also on the type of biosorbent, and follow the order: BC-320 < AB < BC-550. Using the experimental isotherms, the thermodynamic parameters ($\Delta G^0$, $\Delta H^0$ and $\Delta S^0$) for the biosorption of Cu(II) ions on each biosorbent were calculated. The analysis of the obtained values constitutes the main arguments in choosing BC-550 as the most effective biosorbent for the removal of Cu(II) ions from aqueous media.

**Keywords:** biosorption; Cu(II) ions; aqueous media; isotherm modeling; thermodynamic parameters

## 1. Introduction

One of the main problems generated by the development of industrial activities is environmental pollution. The discharge of wastewater, the storage of solid waste, as well as industrial emissions into the air have recently reached alarming levels, precisely due to the intensification and diversification of industrial activities [1,2]. This causes many chemical compounds (such as heavy metal ions, organic molecules and macromolecules, etc.) to reach the environment and contribute significantly to the deterioration of natural ecosystems.

Unlike organic pollutants, the presence of heavy metal ions in the environment has particularly serious consequences for the health of living organisms, due to the fact that these pollutants are non-biodegradable (they accumulate over time), persistent (they are

not destroyed in the environment) and have high mobility (they can contaminate natural ecosystems over quite large distance) [3,4]. Since the elimination of heavy metal ions from industrial processes is practically impossible, due to their economic importance (ex. alloys and electroplating industry, painting and dyeing industry, textile industry, chemical fertilizers manufacturing, etc.) [5,6], the only viable solution is the development of methods for their removal from industrial effluents, thus limiting the negative consequences on the environment.

Various treatment methods are reported in the literature for the treatment of industrial effluents containing heavy metal ions before their discharging into water sources, such as precipitation, coagulation-flocculation, ultra- and nano-filtration, ion exchange, solvent extraction, etc. [7–10]. Unfortunately, most of these methods require a large consumption of materials, energy and time, which makes them inaccessible to small companies that generate various amounts of effluents in which the concentration of metal ions can vary significantly. Compared to these, biosorption, which involves the retention of metal ions on the surface of a solid material called a biosorbent [8,9], is considered an effective, cheap and ecological method, which can be easily adapted to treat variable volumes of effluent [9]. Therefore, biosorption offers a viable alternative for metal ions removal on an industrial scale, which, due to its technological and environmental performance, may become an important method in environmental decontamination processes.

Two aspects must be considered to highlight the practical applicability of biosorption processes in the treatment of industrial effluents. The first is related to the nature of the solid material used as biosorbent. In general, the biosorbent must be a material available in large quantities, easy to prepare and stable over time. Algae biomass fully meets these conditions. Numerous studies in the literature have shown that algae biomass (regardless of their nature) can retain various metal ions from aqueous media, which can then be quantitatively recovered by desorption [10–15]. Unfortunately, in many cases, the biosorption capacity of algae biomass is quite modest [16,17], and this makes efficient removal of metal ions require two or more biosorption steps. A solution to this problem can be the transformation of algae biomass into biochar, through pyrolysis. In the case of algae biomass, pyrolysis can be carried out at relatively low temperatures (up to 600 °C, in an oxygen-poor atmosphere), and the obtained biochar, in addition to a porous structure, also presents numerous superficial functional groups, which can interact with metal ions in aqueous solution [18–20].

The second important aspect in determining the applicability of biosorption processes is to establish the mechanism by which the retention of metal ions occurs. It is well known that the retention of metal ions from aqueous solution by biosorption can be achieved by three distinct mechanisms: ion exchange, superficial complexation and superficial precipitation [21–23]. Establishing the predominant mechanism by which the biosorption of metal ions occurs is a key point from a practical point of view, as it allows the development of an effective strategy for the retention and then recovery of metal ions from industrial effluents. For example, if in the case of the ion exchange mechanism the retention of metal ions requires a short contact time (10–60 min) and their desorption is achieved by using mineral acids (HCl, $HNO_3$, $HClO_4$, etc.) as elluents [24], in the case of the superficial complexation mechanism or the superficial precipitation mechanism, the contact time is much longer (120–240 min) and the desorption of metal ions is achieved, in most of cases, by treatment with a selective complexing agent (such as EDTA) [25]. Determining the thermodynamic parameters of a given biosorption process is a useful tool in establishing the biosorption mechanism in metal ions removal. Thus, based on the Gibbs free energy value ($\Delta G^0$), it can be established whether the biosorption process is favorable or not. This is important in determining its efficiency, especially when treating effluents with high metal ion content [26]. The enthalpy values ($\Delta H^0$) can be correlated with the nature of the interactions that take place during the biosorption process, and allow establishing the temperature regime that can increase the biosorption efficiency [26,27]. Also, the entropy change ($\Delta S^0$) shows whether the biosorption process occurs spontaneously or

not [27]. Therefore, the thermodynamic parameters ($\Delta G^0$, $\Delta H^0$ and $\Delta S^0$) are indicators of the possible nature of metal ions biosorption [28].

Based on these considerations, this study examined the biosorption of Cu(II) ions from aqueous solution onto algae biomass (AB) and biochars obtained from it at 320 °C (BC-320) and 550 °C (BC-550). Batch experiments were performed at different values of contact time, initial metal ion concentration and temperature for all biosorbents. The modeling of the experimental data and the determination of the thermodynamic parameters characteristic of the biosorption processes allow the choice of the most suitable biosorbent for the removal of Cu(II) ions from aqueous media.

## 2. Materials and Methods

### 2.1. Materials

Marine green algae (*Ulva lactuca* sp.) were collected from the Romanian coast of the Black Sea, in August 2021. After repeated washing with tap water (to remove sand and shell impurities) and distilled water (to remove the salts from the surface of the algae leaves), the algae biomass (AB) was air-dried (70 °C, 24 h), ground, sieved and stored in desiccators (to kept its moisture constant). The two biochars were obtained under oxygen-poor atmosphere, at two temperatures of 320 and 550 °C, in a muffle furnace (Nabertherm, Germany). For the preparation of biochars, the algae biomass was transferred into porcelain crucible and placed in the muffle furnace. The pyrolysis time of the algae biomass was 6 h, timed after reaching the desired temperature values (320 and 550 °C). The obtained biochar samples (BC-320 and BC-550) were then cooled in air (to room temperature), mortared and stored in desiccators. The detailed characterization of these biosorbents has been reported in a previous study [29].

A stock solution of Cu(II) ions (650 mg Cu(II)/L) was obtained by dissolving $CuSO_4$ solid salt in distilled water. All working solutions were prepared by diluting the stock solution with distilled water. Fresh solutions were prepared for each experiment.

### 2.2. Biosorbents Characterization

For the characterization of the biosorbents (AB, BC-320 and BC-550), two instrumental methods were used. The first method is FTIR spectrometry (Bio-Rad Spectrometer, (Berlin, Germany), resolution of 4 $cm^{-1}$, spectral range of 400–4000 $cm^{-1}$, KBr pellet technique), which is useful in identifying the nature of the functional groups on the biosorbent surface. The second method is SEM microscopy (SEM Hitachi S3000N (Tokyo, Japan), 20 kV), which allows the morphological analysis of the biosorbent surface. In each case, biosorbent samples were used that were previously dried at 105 °C for 4 h, to obtain constant moisture content.

### 2.3. Biosorption Experiments

All biosorption experiments were performed in batch systems, with intermittent stirring. For kinetic study, 25 mL of Cu(II) ions solution (25.47 mg/L and pH of 5.0) were mixed with 4.0 g/L of each biosorbent, at 25 °C, and a contact time between 5 and 180 min. The experimental conditions: pH of 5.0 and 4.0 g biosorbent/L were established as optimal in a previous study [29]. For isotherm experiments, 25 mL of Cu(II) ions solution ($c_0$ = 12.73–152.83 mg/L) and initial pH of 5.0, were mixed with 4.0 g/L biosorbent (AB, BC-320 and BC-550), for a contact time of 3 h. The same set of experiments was prepared for each temperature value (10, 30 and 50 °C). At the end of biosorption procedure, the samples were filtered (on quantitative filter paper), and Cu(II) ions concentration in the final solutions was analyzed spectrophotometrically (Digital Spectrophotometer S 104D (Haryana, India), rubeanic acid, λ = 390 nm, blank solution), using a prepared calibration graph. The obtained results were used to calculate the characteristic parameters of the biosorption process, namely: biosorption capacity (*q*, mg/g) and removal percent (*R*, %), according to the equations:

$$q = \frac{(c_0 - c) \cdot V}{m} \tag{1}$$

$$R = \frac{c_0 - c}{c_0} \cdot 100 \tag{2}$$

where: $c_o$ and c are the initial and final concentration of Cu(II) ions in solution (mg/L); $V$ is volume of solution (L), and $m$ is the mass of biosorbent used for each experiment (g).

The initial and final pH of aqueous solutions was measured with a pH/ion meter (MM-473 type), equipped with a combined glass electrode.

All the experiments were performed in triplicate, and the mean value of the experimental results was used for calculations and in the graphical representations. All results were analyzed by ANOVA, and $p$-values less than 0.05 were considered significant.

### 2.4. Modeling of Experimental Data

The experimental kinetic data were analyzed using pseudo-first order (Equation (3), pseudo-second order (Equation (4)) and intra-particle diffusion (Equation (5)) models, and the mathematical equations of these models are [30–32]:

$$\log(q_e - q_t) = \log q_e - k_1 \cdot t \tag{3}$$

$$\frac{t}{q_t} = \frac{1}{k_2 \cdot q_e^2} + \frac{t}{q_e} \tag{4}$$

$$q_t = k_{diff} \cdot t^{1/2} + c \tag{5}$$

where: $q_e$ and $q_t$ are biosorption capacity at equilibrium and at time $t$, (mg/g); $k_1$ is the rate constant of pseudo-first order model, (1/min); $k_2$ is the rate constant of pseudo-second order model, (g/mg min); $k_{diff}$ is the intra-particle diffusion rate constant, (mg/g min$^{1/2}$), $c$ is the concentration of Cu(II) ions in solution, (mmol/L).

These models are useful in establishing the rate-determining step of the biosorption process [32] and allow determining the elementary process controlling the retention of Cu(II) ions on the three biosorbents.

To model the equilibrium experimental data, two isotherm models (Langmuir (Equation (6)) and Freundlich (Equation (7)) models) were selected to highlight how Cu(II) ions binding occurs on the surface of the three biosorbents. The mathematical equations of these models are [33,34]:

$$\frac{1}{q} = \frac{1}{q_{\max} \cdot K_L} \cdot \frac{1}{c} \tag{6}$$

$$\log q = \log K_F + \frac{1}{n} \cdot \log c \tag{7}$$

where: $q$ is biosorption capacity, (mg/g); $q_{max}$ is maximum biosorption capacity, (mg/g); $K_L$ is Langmuir constant, (L/g); $c$ is equilibrium concentration of Cu(II) ions in solution, (mg/L); $K_F$ is Freundlich constant, (L/g); $n$ is the heterogeneity factor.

The isotherm and kinetic model, which best describe the experimental data, was selected using the regression coefficients ($R^2$), obtained from the statistical analysis.

The maximum biosorption capacity ($q_{\max}$, mg/g), obtained from the Langmuir model, was then used to calculate the specific surface area occupied by Cu(II) ions retained on each biosorbent ($S$, m$^2$/g), according with the equation [35]:

$$S = \frac{q_{max} \cdot N \cdot M}{A} \tag{8}$$

where: $N$ is the Avogadro number ($6.023 \times 10^{23}$), A is the cross-sectional area of Cu(II) ions ($51.4457 \times 10^{-20}$ m$^2$), and $M$ is the molecular weight of Cu(II) ions (63.456 g/mol).

The thermodynamic parameters: variation of free Gibbs energy ($\Delta G^0$, kJ/mol), variation of enthalpy ($\Delta H^0$, kJ/mol) and variation of entropy ($\Delta S^0$, J/mol K), were calculated using the van't Hoff equations [36,37]:

$$\Delta G^0 = -RT \ln K_e \tag{9}$$

$$\ln K_e = \frac{\Delta H^0}{RT} + \frac{\Delta S^0}{R} \tag{10}$$

$$\Delta S^0 = (\Delta H^0 - \Delta G^0)/T \tag{11}$$

where: $R$ is the universal gas constant (8.314 J/K mol); $T$ is the temperature (K); $K_e$ is the thermodynamic equilibrium constant of biosorption ($K_e = q_e/c_e$).

## 3. Results and Discussion

Although the use of marine algae biomass in metal ions removal processes is well known, their weak mechanical resistance and rather modest biosorption capacity limit the possibility of their large-scale use. Therefore, the transformation of algae biomass into biochar can represent a solution to minimize these disadvantages.

### 3.1. Structural Particularities of the Biosorbents

Since the biosorption process of Cu(II) ions from aqueous media, the nature and number of functional groups on the biosorbents surface are of particular importance, FTIR spectra were recorded for each biosorbent (Figure 1).
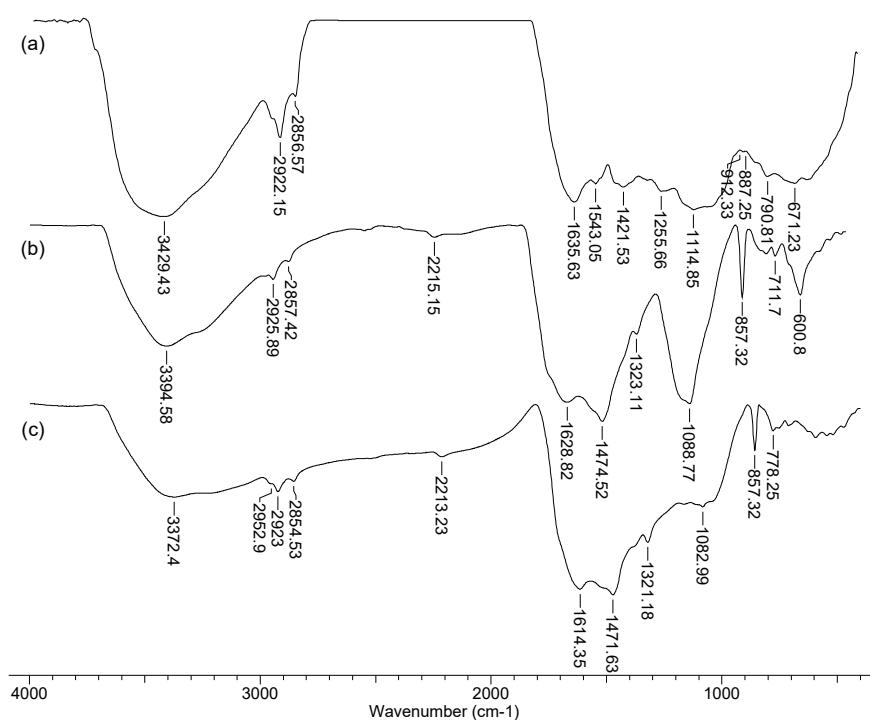


**Figure 1.** FTIR spectra of AB (**a**), BC-320 (**b**) and BC-550 (**c**).

It can be seen (Figure 1) that compared with AB (spectrum a), the number of absorption bands in the case of BC-320 (spectrum b) and BC-550 (spectrum c) is much smaller, and their intensity decrease with the increasing of pyrolysis temperature. However, the presence of absorption bands at 3429–3372 cm$^{-1}$ (characteristic of the O–H bond in alcohols/phenols and of the N–H bond in amines), at 1635–1614 cm$^{-1}$ (attributable to the C=O bond in carbonyl compounds) and at 1114–1082 cm$^{-1}$ (indicating the presence of C–O–C bonds) [38],

show that on the surface of each biosorbent there is a fairly large number of functional groups that can bind Cu(II) ions from aqueous media. On the other hand, increasing the pyrolysis temperature causes both the shift of the absorption bands to lower wave numbers and the appearance of two new absorption bands (Figure 1). The bands at 2215–2213 cm$^{-1}$ and 1323–1321 cm$^{-1}$ (Figure 1, spectra b and c) indicate the presence of multiple bonds (double conjugate or triple) in hydrocarbon radicals and oxygenated compounds [38]. All these observations show that after pyrolysis in the oxygen-limited atmosphere of AB, the degradation of organic molecules from the biomass composition takes place, so that on the surface of the obtained biochars (BC-320 and BC-550), enough functional groups remain that function as binding centers in the biosorption processes.

The morphological changes of the AB surface after pyrolysis at the two values of temperature (320 and 550 °C) were highlighted with the help of SEM images (Figure 2).
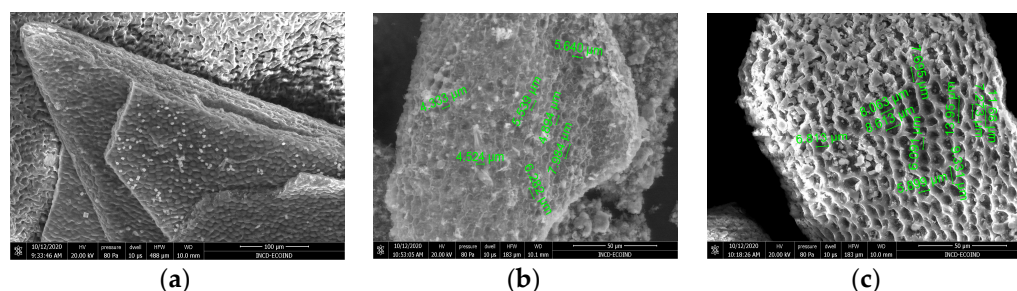


**Figure 2.** SEM images of AB (**a**), BC-320 (**b**) and BC-550 (**c**).

The SEM images illustrated in Figure 2 shows that for both AB and BCs (BC-320 and BC-550), their surface is heterogeneous, irregular and cracked. In addition, the surfaces of BC-320 and BC-550 have a sponge-like appearance (Figure 2b,c), in which the diameter of the free spaces is larger as the pyrolysis temperature is higher. Thus, if in the case of BC-320, the diameter of the free spaces varies between 4.33 and 7.98 μm (Figure 2b), in the case of BC-550, their diameter can reach up to 13.95 μm (Figure 2c). All these characteristics are particularly important in examining the efficiency of the biosorption process.

*3.2. Kinetics of Cu(II) Ions Biosorption*

In evaluating the applicability of a certain biosorption process, it is necessary to known the elementary processes responsible for the binding of metal ions from aqueous solution to the surface of the solid material. Such useful information is obtained by examining the kinetic curves (q = f(t, min)) and modeling the experimental data.

In this study, the kinetic curves were obtained by measuring the biosorption capacity (q, mg/g) of each biosorbent (AB, BC-320 and BC-550) for Cu(II) ions (25.47 mg/L) as a function of contact time (5–180 min), at a pH of 5.0, biosorbent dose of 4.0 g/L and room temperature (25 °C). The obtained results are presented in Figure 3a. It can be observed that in the first 30 min all biosorption processes reach equilibrium, regardless of the nature of the biosorbent (Figure 3a). At higher values of the contact time, the ratio of biosorption processes is much slower, which suggest that the binding centers have been occupied and the biosorbents reach saturation.

But in this 30 min interval, not all three biosorbents (AB, BC-320 and BC-550) behave the same. The experimental data show that BC-550 reach equilibrium in a much shorter time (10 min), compared with AB and BC-320, which need 30 min to reach saturation. In addition, in the first 10 min BC-550 allows the removal of more than 92% of initial concentration of Cu(II) ions, while in the case of AB and BC-320, after 30 min of contact time, the removal percent of Cu(II) ions is no higher than 80% (79.38% for AB and 72.31% for BC-320). These differences between the removal percent values are maintained over the entire contact time interval, so that after 180 min, the removal percents follow the order: 99.73% (BC-550) > 87.54% (AB) > 74.35% (BC-320). Since the difference between the removal

percents at 30 min and at 180 min is at least 8%, a contact time of 180 min (3 h) was selected to obtain the biosorption isotherms.
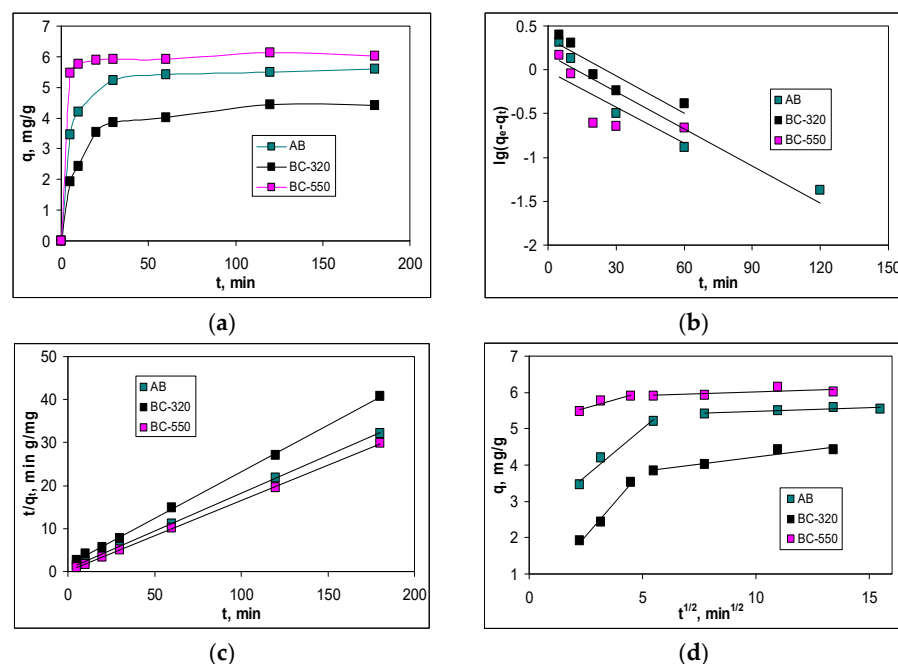


(a)　　　　　　　　　　　　　　(b)



(c)　　　　　　　　　　　　　　(d)

**Figure 3.** Experimental kinetic curves (**a**) and linear representations of pseudo-first order model (**b**), pseudo-second order model (**c**) and intra-particle diffusion model (**d**) for the biosorption of Cu(II) ions on the three biosorbents under mentioned conditions.

All these observations show that among the three biosorbents, BC-550 shows the highest efficiency in the removal of Cu(II) ions from aqueous media (Figure 3a), at least at this value of initial Cu(II) ions concentration (25.47 mg/L). To determine whether the biosorption of Cu(II) ions occurs through chemical interactions with the functional groups of the biosorbents, or only through diffusion within the biosorbent particles, all experimental kinetic curves were modeled using the kinetic models presented in Section 2.4. The linear representations of the three kinetic models (pseudo-first order (PFO), pseudo-second order (PSO) and intra-particle diffusion (IPD) models) for Cu(II) ions biosorption onto the three biosorbents (AB, BC-320 and BC-550) are shown in Figure 3b–d, and the characteristic parameters of these models are summarized in Table 1.

**Table 1.** Kinetic parameters calculated for the biosorption of Cu(II) ions on AB, BC-320 and BC-550, under mentioned experimental conditions.

| Kinetic Model | Parameter | AB | BC-320 | BC-550 |
|---|---|---|---|---|
| PFO | $R^2$ | 0.9069 | 0.8331 | 0.8802 |
| | $q_e$, mg/g | 1.50 | 2.29 | 1.37 |
| | $k_1$, 1/min | 0.0139 | 0.0142 | 0.0137 |
| PSO | $R^2$ | 0.9999 | 0.9994 | 0.9998 |
| | $q_e$, mg/g | 5.67 | 4.62 | 5.93 |
| | $k_2$, g/mg min | 0.0529 | 0.0299 | 0.0609 |
| IPD | $R^2_1$ | 0.9777 | 0.9869 | 0.9046 |
| | $c_1$, mg/L | 2.38 | 2.21 | 5.09 |
| | $k_{diff,1}$, mg/g min$^{1/2}$ | 0.5251 | 0.7321 | 0.1852 |
| | $R^2_2$ | 0.7273 | 0.9068 | 0.9416 |
| | $c_2$, mg/L | 5.27 | 3.44 | 5.81 |
| | $k_{diff,2}$, mg/g min$^{1/2}$ | 0.0201 | 0.0789 | 0.0201 |

It is evident from Table 1 that the highest regression coefficients ($R^2$) were obtained in the case of the pseudo-second order kinetic model (PSO), regardless of the nature of the biosorbent. The good agreement between the experimental data and the pseudo-second order kinetic model (Figure 3c) show that in the studied biosorption processes, the rate-limiting step is the chemical interaction between the Cu(II) ions and the functional groups on the biosorbent surface. Such behavior is characteristic for the retention of metal ions on low-cost materials, and is explained in the literature using the concepts of molecular symmetry [39]. Moreover, for retention on the biosorbents surface, Cu(II) ions need two functional groups, which are geometrically favorable. Since all studied biosorbents (AB, BC-320 and BC-550) have a large number of functional groups on their surface (Figure 1), at this low value of the initial concentration, the retention of Cu(II) ions is rather little influenced by the nature of the biosorbent. However, the rate constants characteristic of the pseudo-second order model (Table 1) increase in the order: BC-320 < AB < BC-550, and this variation can be determined by the surface morphology and the biosorbents (Figure 2).

The pseudo-first order model and the intra-particle diffusion model also describe the experimental data to some extent ($R^2$ = 0.72–0.98). However, it is much more important to emphasize that in the case of the pseudo-first order model, the rate constants have lower values that those obtained for the pseudo-second order model, and their values practically do not depend on the nature of the biosorbent (Figure 3b, Table 1). This suggest that the retention of Cu(II) ions on the surface of biosorbents is dome trough two successive elementary steps: the first—the binding of Cu(II) ions to a functional groups with highest availability, and the second—when the stabilization of the complex formed in the first step takes place, trough chemical interaction with another superficial functional group. The linear representations of the intra-particle diffusion model (Figure 3d) do not pass through the origin and consist of two regions, for all studied biosorbents. This means that elementary diffusion steps contribute to biosorption processes, but are not the rate-limiting steps [34]. And in this case, the values of the kinetic parameters (Table 1) suggest the importance that the morphology of the biosorbent surface has in achieving the biosorption of Cu(II) ions on AB, BC-320 and BC-550.

### 3.3. Isotherms of Cu(II) Ions Biosorption

The variation of the biosorption capacity as a function of the initial metal ions concentration plays an essential role in determining the performance of biosorption processes. These dependencies allow the evaluation of the concentration range in which the biosorbent can retain the metal ions, before reaching saturation [40,41].

Figure 4 shows the dependencies between the biosorption capacity (q, mg/g) and the initial concentration of Cu(II) ions ($c_0$, mg/L), at three different temperatures (10, 30 and 50 °C), for each biosorbent. The other experimental conditions (pH = 5.0, biosorbent dose = 4.0 g/L and contact time = 3 h) were kept the same.
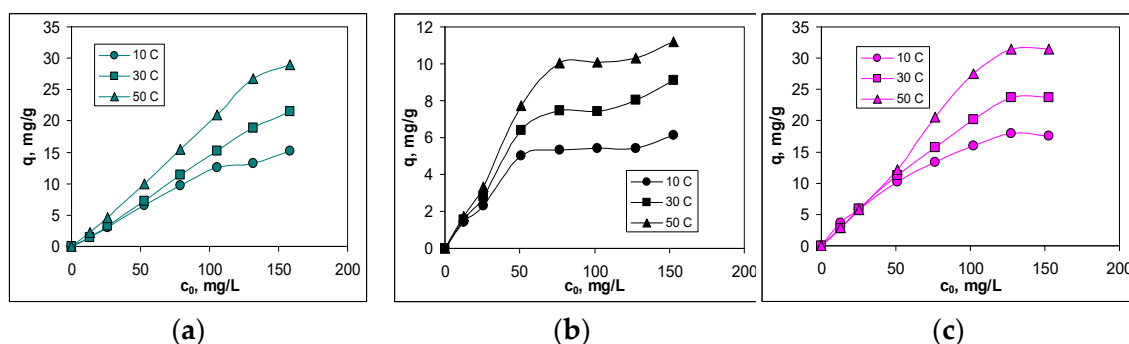


**Figure 4.** Variation of the biosorption capacity (q, mg/g) as a function of initial concentration for the biosorption of Cu(II) ions on AB (**a**), BC-320 (**b**) and BC-550 (**c**).

It can be seen (Figure 4) that for all biosorbents, the biosorption capacity increases with increasing of initial Cu(II) ions concentration and with the increase in temperature. However, if in the case of AB, the variation of the biosorption capacity as a function of the initial Cu(II) ions concentration is almost linear (Figure 4a), in the case of BC-550, saturation of the biosorbents occurs at concentrations higher than 130 mg/L (Figure 4b), while in the case of BC-320, this saturation is observed at much lower Cu(II) ions concentrations (>75 mg/L) (Figure 4c). Also, increasing the temperature from 10 to 50 °C, increases the biosorption capacity (Figure 4), but this improvement is significant only at high concentrations of Cu(II) ions (higher than 100 mg/L). At low initial Cu(II) ions concentrations (up to 50 mg/L), the influence of temperature is less important, regardless of the nature of the biosorbent.

This observation has a particular important practical consequence, namely, in large-scale wastewater treatment increasing temperatures can improve the efficiency of biosorption processes only if the industrial effluent has a high Cu(II) content. If the concentration of Cu(II) in the effluent is low, biosorption can also be carried out at ambient temperature, which significantly reduces the cost of the treatment process.

On the other hand, among the three studied biosorbents, BC-550 has the highest efficiency (compared with AB and BC-320), over entire range of initial Cu(II) ions concentration and at the three temperatures (Figure 4). For example, for the highest initial concentration of Cu(II) ions (153 mg/L) and a temperature of 50 °C, the removal percents increase in the order: BC-320 (35%) < AB (75%) < BC-550 (97%), which shows that BC-550 allows quantitative removal of Cu(II) ions even at high concentrations.

To perform quantitative evaluation of biosorption processes, experimental equilibrium data were analyzed using Langmuir and Freundlich models (Equations (6) and (7)). The linear representations of these models for each biosorbent are illustrated in Figure 5, while the characteristic parameters are summarized in Table 2.

**Table 2.** Langmuir parameters calculated for the biosorption of Cu(II) ions on AB, BC-320 and BC-550, under mentioned experimental conditions.

| Biosorbent | Parameter | 10 °C | 30 °C | 50 °C |
|---|---|---|---|---|
| AB | $R^2$ | 0.9637 | 0.9962 | 0.9879 |
| | $q_{max}$, mg/g | 18.46 | 26.98 | 37.18 |
| | $K_L$, L/g | 0.0063 | 0.0123 | 0.0323 |
| BC-320 | $R^2$ | 0.9669 | 0.9791 | 0.9804 |
| | $q_{max}$, mg/g | 7.73 | 14.84 | 32.31 |
| | $K_L$, L/g | 0.0173 | 0.0182 | 0.0330 |
| BC-550 | $R^2$ | 0.9874 | 0.9887 | 0.9855 |
| | $q_{max}$, mg/g | 20.12 | 25.77 | 55.56 |
| | $K_L$, L/g | 0.1056 | 0.1934 | 0.6135 |

The isotherm experimental data of Cu(II) ions biosorption on AB, BC-320 and BC-550 are best described by the Langmuir isotherm model (Figure 5, Table 2), at all studied temperatures. However, the rather high values of $R^2$ calculated in the case of Freundlich model (Table 3) suggest that the surface of the biosorbents has a high degree of heterogeneity.

Therefore, the retention of Cu(II) ions occurs only on the surface of the biosorbents until a monolayer is formed on their outer surface. The maximum biosorption capacities ($q_{max}$, mg/g) increase with the increasing temperature and follow the order: BC-320 < AB < BC-550 (Table 2). This increase in the maximum biosorption capacity ($q_{max}$, mg/g) is also supported by the values of the specific surface area occupied by Cu(II) ions (Table 4), and indicate that BC-550 is the most effective in retaining Cu(II) ions from aqueous media by biosorption.
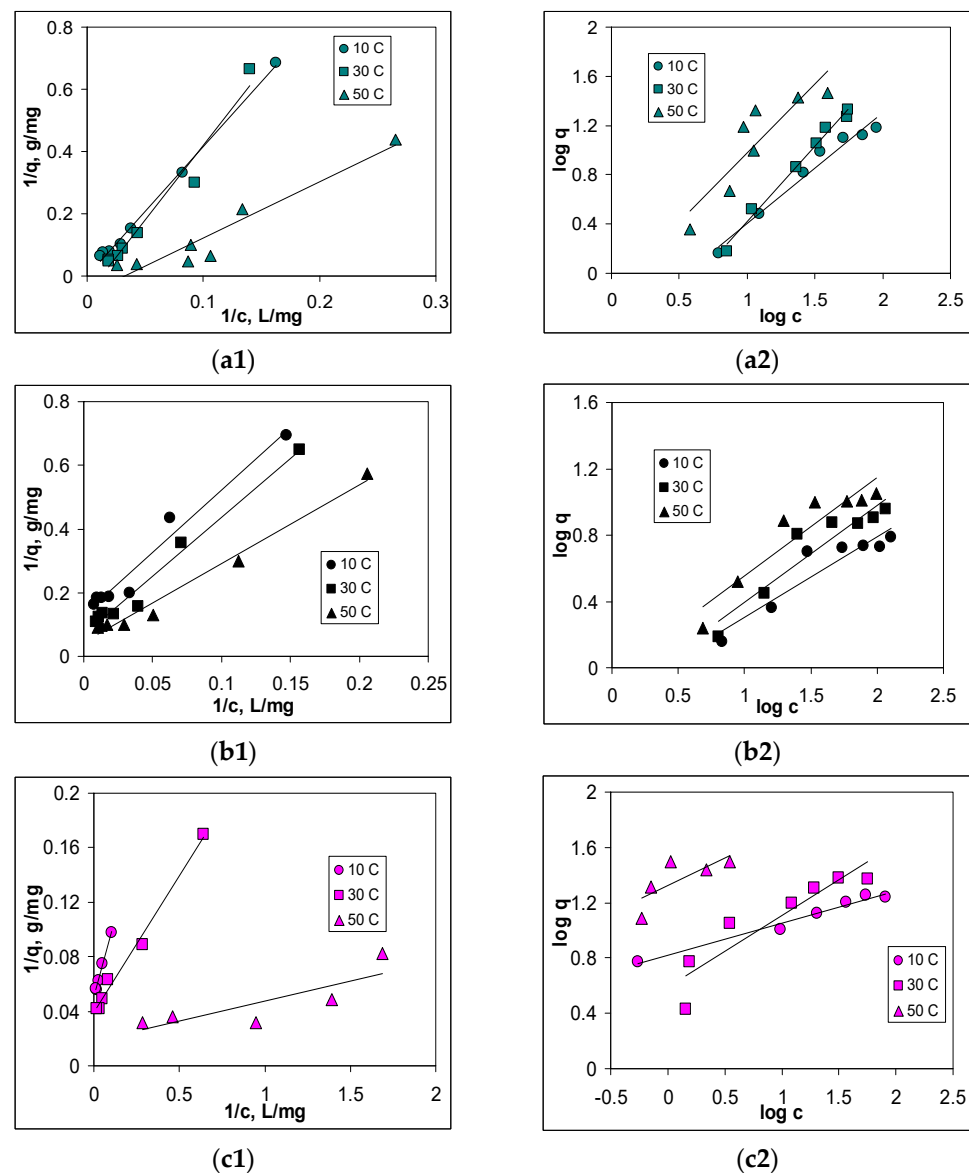
**(a1)**

**(a2)**

**(b1)**

**(b2)**

**(c1)**

**(c2)**

**Figure 5.** Linear representations of Langmuir (**1**) and Freundlich (**2**) models for the biosorption of Cu(II) ions on AB (**a**), BC-320 (**b**) and BC-550 (**c**).

**Table 3.** Freundlich parameters calculated for the biosorption of Cu(II) ions on AB, BC-320 and BC-550, under mentioned experimental conditions.

| Biosorbent | Parameter | 10 °C | 30 °C | 50 °C |
|---|---|---|---|---|
| | $R^2$ | 0.9698 | 0.9879 | 0.7862 |
| AB | n | 1.90 | 1.81 | 1.12 |
| | $K_F$, L/g | 0.3277 | 0.1516 | 0.7409 |
| | $R^2$ | 0.8721 | 0.8877 | 0.8764 |
| BC-320 | n | 2.07 | 1.69 | 1.68 |
| | $K_F$, L/g | 0.6745 | 0.6350 | 0.9084 |
| | $R^2$ | 0.7993 | 0.8470 | 0.8599 |
| BC-550 | n | 4.31 | 2.94 | 2.51 |
| | $K_F$, L/g | 6.6420 | 3.9319 | 2.1101 |

**Table 4.** Specific surface area (S, $m^2/g$) occupied by Cu(II) ions after biosorption on AB, BC-320 and BC-550.

| Biosorbent | 10 °C | 30 °C | 50 °C |
|---|---|---|---|
| AB | 13.73 | 20.07 | 27.66 |
| BC-320 | 5.75 | 11.04 | 24.03 |
| BC-550 | 14.97 | 22.17 | 41.33 |

For a given biosorbent, the values of the Langmuir constant also increase with increasing temperature (Table 2). The Langmuir constant ($K_L$, L/g) is a measure of the strength of the interactions that occurs between the metal ion and the functional groups of the biosorbent during the biosorption [34], and the variation of this parameter shows that all studied biosorption processes are endothermic (being favored by increasing of temperature). On the other hand, the values of the Langmuir constants also depend by the nature of the biosorbent and increase in the order: AB < BC-320 < BC-550 (Table 2). This variation indicates that the Cu(II) ions interact most strongly with the functional groups of BC-550, while in the case of AB, the chemical interactions causing the retention of metal ions are much weaker.

The somewhat different order of the variation of maximum biosorption capacities ($q_{max}$, mg/g) and Langmuir constants ($K_L$, g/L) can be explained if the availability of the superficial functional groups of the biosorbents is taken into account. This in the case of AB, the large number of superficial functional groups and the slightly porous morphology (Figures 1 and 2) make Cu(II) ions to be retained in rather large amounts, but many of these interactions are of a physical nature (most likely hydrogen binds, in which water molecules that hydrate the Cu(II) ions are involved). Consequently, for this biosorbents $q_{max}$ values are high, but $K_L$ values are low. When pyrolysis is carried out at low temperature (the case of BC-320), the partial degradation of the polysaccharides in the cell walls of algae biomass take place, which leads to a decrease in the number of functional groups and to obtaining a surface with a slightly higher porosity (Figures 1 and 2). Therefore, in this case small values of $q_{max}$ but slightly higher values of $K_L$ are obtained, compared with AB. In the case of BC-550 (biochar obtained at high pyrolysis temperature), the advanced degradation of cell walls allows obtaining a materials with a high degree of porosity (Figures 1 and 2). In these cavities Cu(II) ions can easily penetrate and bind through strong (chemical) interactions. Thus, in the case of BC-550, both $q_{max}$ and $K_L$ have the highest values (compared to AB and BC-320).
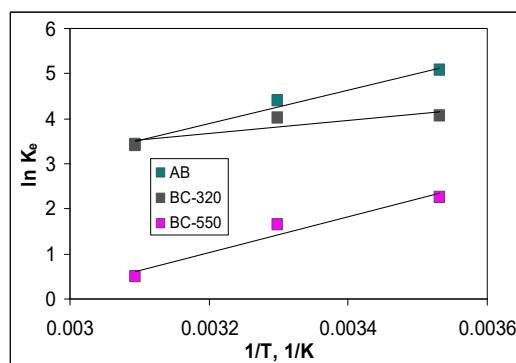
Regarding the Freundlich isotherm, the values obtained for parameter n were greater than 1.0, indicating favorable conditions for biosorption and a high affinity between the biosorbent and Cu(II) ions, which facilitates chemisorptions.

### 3.4. Thermodynamic Parameters of Cu(II) Ions Biosorption

As shown in the previous section, increasing of temperature (from 10 to 50 °C) causes an increase in biosorption capacity of 91% for AB, 81% for BC-320 and 79.97% for BC-550 (Figure 4), which indicate that the biosorption processes are endothermic, regardless the nature of the biosorbent. Therefore, for the thermodynamic characterization of the retention of Cu(II) ions on the three biosorbents (AB, BC-320 and BC-550), the thermodynamic parameters were calculated (using Equations (9)–(11)). The values of the thermodynamic parameters ($\Delta G^0$, $\Delta H^0$ and $\Delta S^0$) obtained for the biosorption of Cu(II) ions on AB, BC-320 and BC-550, are presented in Table 5, and the linear dependencies ln $K_e$ vs. $1/T$ (required to calculate $\Delta H^0$ and $\Delta S^0$) are illustrated in Figure 6.

**Table 5.** Thermodynamic parameters for Cu(II) ions biosorption on AB, BC-320 and BC-550.

| Biosorbent | Temperature, °C | $\Delta G^0$, kJ/mol | $\Delta H^0$, kJ/mol | $\Delta S^0$, kJ/mol K |
|---|---|---|---|---|
| AB | 10 | −11.93 | | |
| | 30 | −11.09 | 11.47 | 0.96 |
| | 50 | −9.22 | | |
| BC-320 | 10 | −10.09 | | |
| | 30 | −9.55 | 10.02 | 1.16 |
| | 50 | −9.16 | | |
| BC-550 | 10 | −15.29 | | |
| | 30 | −14.14 | 7.98 | 1.41 |
| | 50 | −13.13 | | |



**Figure 6.** $lnK_e$ vs. 1/T dependencies for the biosorption of Cu(II) ions on the three biosorbents.

The negative values of the Gibbs free energy ($\Delta G^0$) indicate that the biosorption of Cu(II) ions is a spontaneous process regardless the nature of the biosorbent, in the studied temperature range. However, the values of $\Delta G^0$ (Table 5) increase in the order: BC-550 < AB < BC-320, which show that BC-550 has the highest affinity for Cu(II) ions in aqueous media. This observation is consistent with the experimental results presented in the previous sections.

On the other hand, increasing the temperature in the range 10–50 °C causes an insignificant increase in the $\Delta G^0$ values (2.71 kJ/mol for AB, 0.93 kJ/mol for BC-320 and 2.16 kJ/mol for BC-550) (Table 5). However, such behavior shows that increasing the temperature requires less energy to carry out the biosorption process, and this is characteristic of endothermic processes [42]. Therefore, the nature of interactions occurring in the biosorption process of Cu(II) ions does not change with the temperature variation, and that they are predominantly chemical in nature.

The endothermic nature of the biosorption processes of Cu(II) ions on AB, BC-320 and BC-550 is also demonstrated by the positive values of the $\Delta H^0$. The variation of this parameters for the biosorption of Cu(II) ions follow the order: BC-550 < BC-320 < AB (Table 5), which show that the energy consumed for the retention of metal ions is the lowest in the case of BC-550. Therefore in the case of this biosorbent, the functional groups have the highest availability to interact with Cu(II) ions in aqueous media. This observation is also consistent with the experimental results presented above. According to the literature studies, a $\Delta H^0$ value between 2 and 20 kJ/mol indicates a physical biosorption process, while a $\Delta H^0$ value between 80 and 200 kJ/mol is chemical in nature [43]. In the case of Cu(II) ions biosorption on AB, BC-320 and BC-550, the $\Delta H^0$ values varied between 11.47 and 7.98 kJ/mol. However, biosorption processes cannot be considered physical in nature (taking into account the observations presented above). Most likely, the interactions between metal ions and functional groups of the biosorbents are electrostatic (ion-exchange type), which explains the values obtained for both $\Delta H^0$ and $\Delta G^0$.

The existence of predominantly electrostatic interactions in Cu(II) ions biosorption processes is also supported by the small and positive $\Delta S^0$ values (Table 5). These positive

values indicate the affinity of Cu(II) ions for the functional groups of the biosorbents. However, the low values of this parameter show that during of the biosorption processes, the randomness at the liquid/solid interface varies a quite little. This behavior is characteristic of ion exchange processes [44], where the binding of a metal ion (Cu(II) in this case) occurs simultaneously with the release of another mobile ion into solution, according to the equilibrium:

$$Biosorbent - M + Cu^{2+} \leftrightarrows Biosorbent - Cu + M^{2+} \tag{12}$$

where: M is the mobile ion.

Most likely, the mobile ion in ion exchange processes is Ca(II). This observation is based on: (i) in the chemical composition of each biosorbent, the Ca(II) content is significant (2.96% for AB, 5.79% for BC-320, and 7.62% for BC-550 [29]), (ii) the ionic radius of Ca(II) ion (174 pm) is higher than the ionic radius of Cu(II) ions (138 pm), and (iii) the pH measured in aqueous solution after biosorption increase slightly (from 5.0 to 5.31 for AB, from 5.0 to 5.42 for BC-320, and from 5.0 to 6.20 for BC-550), suggesting the formation of a basic compound in solution.

All the discussions included in this study show that the transformation of marine algae biomass into biochar can represent a solution for obtaining biosorbents with high efficiency in metal ion biosorption processes. However, the temperature at which pyrolysis is performed must be carefully chosen so that obtained biochar has a porous structure that facilitates interactions between metal ions and surface functional groups. Precisely for this reason, the pyrolysis of algae biomass at 550 °C, although it is more expensive (compared to pyrolysis at 320 °C), allows obtaining a biosorbent with better kinetic, equilibrium and thermodynamic characteristics in the biosorption process of Cu(II) ions from aqueous media.

## 4. Conclusions

In this study, marine green algae biomass (*Ulva lactuca* sp.) (AB) and the biochars obtained at two different temperatures (BC-320 and BC-550) were used as biosorbents for the removal of Cu(II) ions from aqueous solution. The obtained experimental results showed that BC-550 has better biosorption performance for Cu(II) ions compared with the other biosorbents (AB and BC-320). The kinetic data are best described by the pseudo-second order kinetic model, while the equilibrium data follow the Langmuir model. In addition, the thermodynamic parameters calculated for each case indicate that the biosorption process is spontaneous and feasible regardless the nature of the biosorbent. This indicates that the retention of Cu(II) ions is achieved through electrostatic interactions that take place on the surface of the biosorbent until a monolayer coverage is formed. Therefore, the superficial functional groups and the surface morphology of the biosorbent play an important role in the development of the biosorption processes. All these observations show that the transformation of marine algae biomass into biochar can represent a solution for obtaining biosorbents with high efficiency in metal ion biosorption processes, which can be used for large-scale applications.

# References

1. Sarode, S.; Upadhyay, P.; Khosa, M.A.; Mak, T.; Shakir, A.; Song, S.; Ullah, A. Overview of wastewater treatment methods with special focus on biopolymer chitin-chitosan. *Int. J. Biol. Macromol.* **2019**, *121*, 1086–1100. [CrossRef] [PubMed]
2. Crini, G.; Lichtfouse, E. Advantages and disadvantages of techniques used for wastewater treatment. *Environm. Chem. Lett.* **2019**, *17*, 145–155. [CrossRef]
3. Nowicka, B. Heavy metal—Induced stress in eukaryotic algae—Mechanisms of heavy metal toxicity and tolerance with particular emphasis on oxidative stress in exposed cells and the role of antioxidant response. *Environ. Sci. Poll. Res.* **2022**, *29*, 16860–16911. [CrossRef] [PubMed]
4. Ackova, D.G. Heavy metals and their general toxicity on plants. *Plant Sci. Today* **2018**, *5*, 15–19.
5. Behera, M.; Nayak, J.; Banerjee, S.; Chakrabortty, S.; Tripathy, S.K. A review on the treatment of textile industry waste effluents towards the development of efficient mitigation strategy: An integrated system design approach. *J. Environ. Chem. Eng.* **2021**, *9*, 105277. [CrossRef]
6. Varjani, S.; Joshi, R.; Srivastava, V.K.; Ngo, H.H.; Guo, W. Treatment of wastewater from petroleum industry: Current practices and perspectives. *Environ. Sci. Poll. Res.* **2020**, *27*, 27172–27180. [CrossRef] [PubMed]
7. Bashir, A.; Malik, L.A.; Ahad, S.; Manzoor, T.; Bhat, M.A.; Dar, G.N.; Pandith, A.H. Removal of heavy metal ions from aqueous system by ion-exchange and biosorption methods. *Environ. Chem. Lett.* **2019**, *17*, 729–754. [CrossRef]
8. Saleh, T.A.; Mustaqeem, M.; Khaled, M. Water treatment technologies in removing heavy metal ions from wastewater: A review. *Environ. Nanotechn. Monit. Manag.* **2022**, *17*, 100617. [CrossRef]
9. Vijayaraghavan, K.; Balasubramanian, R. Is biosorption suitable for decontamination of metal-bearing wastewaters? A critical review on the state-of-the-art of biosorption processes and future directions. *J. Environ. Manag.* **2015**, *160*, 283–296. [CrossRef]
10. Crini, G.; Lichtfouse, E.; Wilson, L.D.; Morin-Crini, N. Conventional and non-conventional adsorbents for wastewater treatment. *Environ. Chem. Lett.* **2019**, *17*, 195–213. [CrossRef]
11. Cheng, S.Y.; Show, P.L.; Lau, B.F.; Chang, J.S.; Ling, T.C. New Prospects for Modified Algae in Heavy Metal Adsorption. *Trends Biotechnol.* **2019**, *37*, 1255–1268. [CrossRef]
12. El-Sayed, S.; Hyun-Seog, R.; Subhabrata, D.; Moonis, A.K.; Abou-Shanab, R.A.I.; Chang, S.W.; Jeon, B.H. Algae as a green technology for heavy metals removal from various wastewater. *World J. Microbiol. Biotechnol.* **2019**, *35*, 75–94.
13. Fawzy, M.A. Biosorption of copper ions from aqueous solution by *Codium vermilara*: Optimization, kinetic, isotherm and thermodynamic studies. *Adv. Power Technol.* **2020**, *31*, 3724–3735.
14. Li, R.; Zhang, T.; Zhong, H.; Song, W.; Zhou, Y.; Yin, X. Bioadsorbents from algae residues for heavy metal ions adsorption: Chemical modification, adsorption behaviour and mechanism. *Environ. Technol.* **2021**, *42*, 3132–3143. [CrossRef] [PubMed]
15. Ramesh, B.; Saravanan, A.; Senthil Kumar, P.; Yaashikaa, P.R.; Thamarai, P.; Shaji, A.; Rangasamy, G. A review on algae biosorption for the removal of hazardous pollutants from wastewater: Limiting factors, prospects and recommendations. *Environ. Poll.* **2023**, *327*, 121572. [CrossRef] [PubMed]
16. Jayakumar, V.; Govindaradjane, S.; Rajamohan, N.; Rajasimman, M. Biosorption potential of brown algae, *Sargassum polycystum*, for the removal of toxic metals, cadmium and zinc. *Environ. Sci. Poll. Res.* **2022**, *29*, 41909–41922. [CrossRef]
17. Dulla, J.B.; Tamana, M.R.; Boddu, S.; Pulipati, K.; Srirama, K. Biosorption of copper(II) onto spent biomass of *Gelidiella acerosa* (brown marine algae): Optimization and kinetic studies. *Appl. Water Sci.* **2020**, *10*, 56–66. [CrossRef]
18. Liu, Z.; Xu, Z.; Xu, L.; Buyong, F.; Chay, T.C.; Cai, Y.; Hu, B.; Zhu, Y.; Wang, X. Modifed biochar: Synthesis and mechanism for removal of environmental heavy metals. *Carbon Res.* **2022**, *1*, 8–29. [CrossRef]
19. Tomczyk, A.; Sokołowska, Z.; Bogut, P. Biochar physicochemical properties: Pyrolysis temperature and feedstock kind effects. *Rev. Environ. Sci. Biotechnol.* **2020**, *19*, 191–215. [CrossRef]
20. Khan, A.A.; Gul, J.; Naqvi, S.R.; Ali, J.; Farooq, W.; Liaqat, R.; Al Mohamadi, H.; Stepanec, L.; Juchelkov, D. Recent progress in microalgae-derived biochar for the treatment of textile industry wastewater. *Chemosphere* **2022**, *306*, 135565. [CrossRef]
21. Gupta, S.; Sireesha, S.; Sreedhar, I.; Patel, C.M.; Anitha, K.L. Latest trends in heavy metal removal from wastewater by biochar based sorbents. *J. Water. Proc. Eng.* **2020**, *38*, 101561. [CrossRef]
22. Singh, A.; Sharma, R.; Pant, D.; Malaviya, P. Engineered algal biochar for contaminant remediation and electrochemical applications. *Sci. Total Environ.* **2021**, *774*, 145676. [CrossRef]
23. Khandgave, S.S.; Sreedhar, I. A mini-review on engineered biochars as emerging adsorbents in heavy metal removal. *Mat. Today Proc.* **2023**, *72*, 19–26. [CrossRef]
24. Wu, J.; Wang, T.; Wang, J.; Zhang, Y.; Pan, W.P. A novel modified method for the efficient removal of Pb and Cd from wastewater by biochar: Enhanced the ion exchange and precipitation capacity. *Sci. Total Environ.* **2021**, *754*, 142150. [CrossRef] [PubMed]
25. Wang, S.; Kwak, J.H.; Islam, S.; Naeth, M.A.; El-Din, M.G.; Chang, S.X. Biochar surface complexation and Ni(II), Cu(II), and Cd(II) adsorption in aqueous solutions depend on feedstock type. *Sci. Total Environ.* **2020**, *712*, 136538. [CrossRef]
26. Foroutan, R.; Mohammadi, R.; Farjadfard, S.; Esmaeili, H.; Saberi, M.; Sahebi, S.; Dobaradaran, S.; Ramavandi, B. Characteristics and performance of Cd, Ni, and Pb bio-adsorption using Callinectes sapidus biomass: Real wastewater treatment. *Environ. Sci. Poll. Res.* **2019**, *26*, 6336–6347. [CrossRef]
27. Chen, T.; Da, T.; Ma, Y. Reasonable calculation of the thermodynamic parameters from adsorption equilibrium constant. *J. Molec. Liq.* **2021**, *322*, 114980. [CrossRef]

28. Moreira, V.R.; Lebron, Y.A.R.; Freire, S.J.; Santos, L.V.S.; Palladino, F.; Jacob, R.S. Biosorption of copper ions from aqueous solution using *Chlorella pyrenoidosa*: Optimization, equilibrium and kinetics studies. *Microchem. J.* **2019**, *145*, 119–129. [CrossRef]

29. Ciobanu, A.A.; Munteanu, L.; Vasile, G.; Bulgariu, L. Evaluation of the biosorption performance of marine green algae biomass (*Ulva lactuca* sp.) in the removal of inorganic pollutants. *Bull. IP Iasi* **2023**, *69*, 93–104.

30. Ho, Y.S.; McKay, G. Pseudo-second-order model for sorption processes. *Process Biochem.* **1999**, *34*, 451–465. [CrossRef]

31. Wang, J.; Guo, X. Rethinking of the intraparticle diffusion adsorption kinetics model: Interpretation, solving methods and applications. *Chemosphere* **2022**, *309*, 136732. [PubMed]

32. Tan, K.L.; Hameed, B.H. Insight into the adsorption kinetics models for the removal of contaminants from aqueous solutions. *J. Taiwan Inst. Chem. Eng.* **2017**, *74*, 25–48. [CrossRef]

33. Chong, K.H.; Volesky, B. Description of two-metal biosorption equilibria by Langmuir-type models. *Biotechnol. Bioeng.* **1995**, *47*, 451–460. [CrossRef]

34. Rangabhashiyam, S.; Anu, N.; Nandagopal Giri, M.S.; Selvaraju, N. Relevance of isotherm models in biosorption of pollutants by agricultural by-products. *J. Environ. Chem. Eng.* **2014**, *2*, 398–414. [CrossRef]

35. Ozer, A.; Ozer, D.; Ozer, A. The adsorption of copper (II) ions on dehydrated wheat bran: Determination of the equilibrium and thermodynamic parameter. *Process Biochem.* **2004**, *39*, 2183–2191. [CrossRef]

36. Lima, E.C.; Gomes, A.A.; Tran, H.N. Comparison of the nonlinear and linear forms of the van't Hoff equation for calculation of adsorption thermodynamic parameters ($\Delta S°$ and $\Delta H°$). *J. Molec. Liq.* **2020**, *311*, 113315. [CrossRef]

37. Sahmoune, M.N. Evaluation of thermodynamic parameters for adsorption of heavy metals by green adsorbents. *Environ. Chem. Lett.* **2019**, *17*, 697–704. [CrossRef]

38. Dean, J.A. *Handbook of Analytical Chemistry*; Mc-Grow Hill Inc.: New York, NY, USA, 1995.

39. Russo, F.; Tenore, A.; Mattei, M.R.; Frunzo, L. A Mathematical Study of Metal Biosorption on Algal–Bacterial Granular Biofilms. *Bull. Mathem. Biol.* **2023**, *85*, 63. [CrossRef]

40. Syeda, H.I.; Sultan, I.; Razavi, K.S.; Yap, P.S. Biosorption of heavy metals from aqueous solution by various chemically modified agricultural wastes: A review. *J. Water. Proc. Eng.* **2022**, *46*, 102446. [CrossRef]

41. Yang, X.; Wan, Y.; Zheng, Y.; He, F.; Yu, Z.; Huang, J.; Wang, H.; Ok, S.; Jiang, Y.; Gao, B. Surface functional groups of carbon-based adsorbents and their roles in the removal of heavy metals from aqueous solutions: A critical review. *Chem. Eng. J.* **2019**, *366*, 608–621. [CrossRef]

42. Menezes, J.M.C.; da Silva Bento, A.M.; de Paula Filho, F.J.; da Costa, J.G.M.; Melo Coutinho, H.D.; Pereira Teixeira, R.N. Kinetic and thermodynamic study of copper (II) IONS biosorption by *Caryocar coriaceum* Wittm bark. *Sustain. Chem. Pharm.* **2021**, *19*, 100364. [CrossRef]

43. Menezes, J.M.C.; da Silva Bento, A.M.; da Silva, J.H.; de Paula Filho, F.J.; da Costa, J.G.M.; Coutinho, H.D.M.; Pereira Teixeira, R.N. Equilibrium, kinetics and thermodynamics of lead (II) adsorption in bioadsorvent composed by *Caryocar coriaceum* Wittm barks. *Chemosphere* **2020**, *261*, 128144. [CrossRef] [PubMed]

44. Kadiri, L.; Lebkiri, A.; Rifi, E.H.; Ouass, A.; Essaadaoui, Y.; Lebkiri, I. Mathematical modeling and thermodynamic study of copper (II) removal from aqueous solution by Coriandrum Sativum seeds. *Mediterr. J. Chem.* **2019**, *7*, 478–490. [CrossRef]